Available online at www.sciencedirect.com
ScienceDirect
Ceramics International 36 (2010) 1357–1364
CERAMICS INTERNATIONAL
www.elsevier.com/locate/ceramint

A novel colloidal processing route to alumina ceramics

Ibram Ganesh [a,*], G. Sundararajan [a], Susana M. Olhero [b], Paula M.C. Torres [c], José M.F. Ferreira [c]

[a] Centre for Advanced Ceramics, International Advanced Research Centre for Powder Metallurgy and New Materials (ARCI), Hyderabad 500005, Andhra Pradesh, India
[b] Department of Mechanical Engineering and Industrial Management, FEUP, University of Porto, Porto, Portugal
[c] Department of Ceramics and Glass Engineering, CICECO, University of Aveiro, Aveiro P-3810193, Portugal

Received 8 October 2009; received in revised form 26 November 2009; accepted 7 January 2010
Available online 29 January 2010

Abstract

The fabrication of complex-shaped alumina ceramics following a new near-net shape technique based on hydrolysis induced aqueous gelcasting (GCHAS) is reported in this paper. Aqueous suspension containing 50 vol.% solids loading was prepared by dispersing alumina in an aqueous solution of methacrylamide and methlynebisacrylamide (17 wt.% in 6:1) using polycarboxylic acid as dispersing agent. Consolidation was accomplished by adding a polymerization initiator, a catalyst and AlN powder (4 wt.%). For comparison purposes, alumina ceramics were also consolidated by aqueous gelcasting (GC) and by hydrolysis assisted solidification (HAS) from the same concentrated suspensions, and by conventional dry pressing (DP) from freeze dried granules prepared from the same suspensions by freeze granulation. Among the four shaping techniques used, GCHAS was found to be best for consolidating near-net shape alumina components like thin wall radomes with the highest green strength ever reported for alumina ceramics. Green samples were sintered for 2 h at 1600 °C and then characterized for microstructure and mechanical properties.

Keywords: Alumina; Gelcasting; Hydrolysis assisted solidification; Hydrolysis induced aqueous gelcasting; Rheology; Near-net shape; Radome

1. Introduction

Alumina is one of the most investigated ceramic materials owing to its widespread industrial applications and because of its high quality/price ratio [1–4]. It has been demonstrated that the final properties of ceramic materials are highly dependent on the processing route and processing variables [5]. This is particularly true for complex-shaped parts in which high density and high uniformity of the microstructure are the key factors. Such demands are easier to achieve by using colloidal shaping techniques than by conventional dry pressing. Colloidal processing routes such as slip casting or pressure slip casting enable an effective break down of particle agglomerates, the control of interaction forces between the dispersed particles and a good packing ability, which, in turn, enhance the sintering ability at lower temperatures, avoiding coarsening of the sintered microstructure and thus improving the reliability of performance [5]. Moreover, a great variety of direct consolidation techniques such as, aqueous gelcasting [6], hydrolysis induced aqueous gelcasting [7], hydrolysis assisted solidification [8], temperature induced forming (TIG) [9], etc., have been developed recently. These techniques enable to preserve in the green bodies the high degree of homogeneity achieved in the suspensions due to absence of liquid removal that in some instances could promote particles segregation [5].

The suitability of aqueous gelcasting for near-net-shaping ceramic parts with relatively high green strength, which enable green machining is well recognized [6,10,11]. Despite several advantages, the main limitation of this process is the high sensitivity of the green parts to drying, namely, they are prone to form cracks during this step. This is even more severe in parts having different cross sections at different places such as in the case of nose and walls of a radome as they often crack due to the involved thermal gradient. To address the problems associated with GC, a new near-net-shaping technique namely, hydrolysis

* Corresponding author. Fax: +91 040 24442699.
E-mail addresses: ibram_ganesh@yahoo.com, ibramganesh@arci.res.in (I. Ganesh).

0272-8842/$36.00
doi:10.1016/j.ceramint.2010.01.022

induced aqueous gelcasting (GCHAS) has been proposed recently [7,12,13]. This new process is a combination of HAS and GC and was found to be a versatile, easy, fast, effective and economic process for consolidating all kinds of aqueous particulate suspensions that have alumina as a major or minor constituent. The synergetic effects of these two processes are quick setting of the suspension into a stiff gel under ambient conditions with an exceptionally high strength and an absence of differential shrinkage during drying, avoiding cracking of the part upon drying as water is partially consumed upon hydrolysis of AlN ($AlN + 2H_2O \rightarrow AlO(OH) + NH_3$). The concomitant increase in pH of the system can also favourably change the permeability of the green bodies and minimize the thermal/moisture gradients.

In view of the above, a systematic study was undertaken to utilize the GCHAS technique to make dense near-net shape alumina ceramics from suspensions containing 50 vol.% alumina. For comparison purposes, the performance of other processing routes: aqueous gelcasting, hydrolysis assisted solidification and dry pressing was also tested in this study. Differently consolidated green samples were sintered for 2 h at 1600 °C. The starting suspensions, green bodies and the sintered ceramics were thoroughly characterized by various techniques. The beneficial effects of aqueous colloidal processing over conventional dry pressing and of GCHAS over other colloidal processing routes are presented and discussed in this paper.

2. Experimental procedure

2.1. Materials and reagents

An alumina powder (CT-3000SG, Alcoa-Chemie GmbH, Ludwigshafen, Germany, with an average particle size, $D_{50} = 0.8$ μm), and a high purity AlN powder (Grade AT, H.C. Stark, Goslar, Germany, $D_{50} = 0.33$ μm, oxygen content < 1.3%) were used in this study as starting raw materials. A polycarboxylic acid without alkalis, Dolapix CE 64 (Zschimmer and Schwarz, Chemnitztalstrasse, Germany) was used as dispersing agent.

2.2. Powder processing routes

2.2.1. Dry powder pressing (DP)

In a typical experiment, initially, a stock suspension with 50 vol.% solids loading was prepared by dispersing the alumina powder in double distilled water using Dolapix CE 64 as a dispersing agent (0.4 wt.% on the dry powder weight basis). De-agglomeration of the powder in the suspension was performed by ball milling for 24 h in a polypropylene bottle using alumina balls (the charge to balls weight ratio was 1:3). Considering that the concentrated (50 vol.%) suspension tended to exhibit shear thickening characteristics under high shear rates, as those prevailing when flowing through the narrow (0.7 mm diameter) spraying nozzle, the aqueous stock suspension was diluted to 35 vol.% before freeze granulation. The required amount of distilled water was added together with 3 wt.% (on the powder weight basis) of an emulsion binder, Duramax D1000 (Rohm and Haas, Lauterbourg, France) as processing aid. The diluted suspension was then freeze granulated by spraying into liquid nitrogen (−196 °C) (Power Pro freeze granulator LS-2, Gothenburg, Sweden). The resultant granules were then dried at −49 °C under a pressure, 1×10^{-3} torr, in a freeze drying system (Labconco, LYPH Lock 4.5, Kansas City, USA) for several days. The dried granules were uni-axially pressed in a metal die by applying a pressure of 200 MPa to obtain pellets with 30 mm diameter × 8 mm height.

2.2.2. Hydrolysis assisted solidification (HAS)

To the stable and de-agglomerated 50 vol.% solids loaded aqueous alumina suspension formed in the DP process, 4 wt.% of AlN (on powder weight basis) together with the required amount of water to keep the total solids loading unchanged were added and ball milling process was continued for further 2 h under the same conditions as employed in the DP process. The resultant suspension was then filtered off and degassed for 3 min by vacuum pumping. This degassed suspension was then cast in split-type white petroleum jelly coated aluminium moulds (60 mm × 30 mm × 30 mm) and was allowed to set under ambient conditions *via* HAS.

2.2.3. Aqueous gelcasting (GC)

In this process, 50 vol.% solids loaded aqueous suspension was prepared by dispersing α-Al_2O_3 in an aqueous-organic premix (CPM, conventional pre-mix solution) solution obtained by dissolving 17 wt.% methacrylamide (MAM) and methylene-bisacrylamide (MBAM) in 6:1 ratio in double distilled water in the presence of the same dispersing agent (0.4 wt.% Dolapix CE 64) [10,11]. After subjecting to de-agglomeration by ball milling for 24 h in a polypropylene bottle using alumina balls (the charge to balls weight ratio was 1:3), the suspension was separated from balls and was added with a de-airing agent (1-octanol at the ratio of 1 μL/g of suspension) to remove the air bubbles from the suspension. This suspension was further subjected to degassing process for 3 min by vacuum pumping. A polymerization initiator (10 wt.% aqueous solution of ammonium per-sulphate, APS) and a catalyst (tetra-methylethylenediammine, TEMED) at the ratio of 4 and 2 μL/g of suspension, respectively [10,11], were then added and the suspension was once again degassed for 2 min prior to casting. The suspension was then poured in non-porous white petroleum jelly coated split-type aluminium moulds (60 mm × 30 mm × 30 mm) and allowed to set under ambient conditions.

2.2.4. Hydrolysis induced aqueous gelcasting (GCHAS)

To the stable and de-agglomerated alumina suspension with 50 vol.% solids loading formed in the above described GC process, 4 wt.% of AlN (on powder weight basis) together with the required amount of water to keep the total solids loading unchanged were added and ball milling was continued for further 2 h. This homogenous suspension was then degassed by vacuum pumping to get rid of air bubbles from it. The same polymerization initiator (APS) and catalyst

(TEMED) used in GC process were added at the ratios of 2 and 1 μL/g of suspension, respectively. The suspension was once again degassed for 2 min prior to casting in a split-type Teflon lined aluminium mould and let to set under ambient conditions after inserting a suitable mandrel to obtain a hollow cone like shape (radome). After gelation (within about 15 min), the mandrel was removed from the part and the mould was filled with water miscible poly(ethylene glycol) 400 (PEG400) (AR grade, Loba-Chemie, Mumbai, India) [14]. Due to the difference in chemical potential, water moves from gel into the PEG solution [14]. After 2 h, the PEG was removed from the mould. At this stage, the radome part was like a strong rubber and it could be removed from the mould easily just by tilting the mould upside down. Small bulk samples (30 mm × 30 mm × 60 mm) were also cast in suitable moulds to check the gelation condition before removing the mandrel and to allow a comparison with the other consolidation techniques.

All green bodies prepared by the various processing routes, including the radome consolidated by GCHAS (Fig. 1) were placed in a humidity controlled oven preset at 40 °C and 90% RH. After 24 h under these conditions, the temperature in the humidity oven was raised to 70 °C and held for further 24 h. The dried samples were heat treated at a rate of 1 °C/min up to 500 °C and held at this temperature for 2 h. Then the sintering was conducted at a heating rate of 5 °C/min up to 1600 °C with 2 h holding time at this temperature.

Fig. 1. A green radome shape (about 290 mm height and 125 mm base diameter) consolidated by hydrolysis induced aqueous gelcasting (GCHAS) of a suspension containing 50 vol.% of alumina + 4 wt.% AlN in a split-type Teflon lined aluminium mould.

2.3. Characterization techniques

Particle size analysis of the powders was performed by using a light scattering equipment (Coulter LS 230, Miami, UK, Fraunhofer optical model). The viscosity of suspensions was measured using a rotational Rheometer (Bohlin C-VOR Instruments, Worcestershire, UK). The measuring configuration adopted was a cone and plate (4°, 40 mm, and gap of 150 μm), and flow measurements were conducted between 0.1 and 200 s^{-1}. Oscillatory measurements were to access the evolution of the internal structure during setting of GC and GCHAS suspensions.

Bulk density (BD), apparent porosity (AP), and water absorption (WA) capacity of various sintered alumina ceramics were measured in water according to Archimedes principle (ASTM C372) using a Mettler balance (AG 245, Mettler Toledo, Switzerland). Three density measurements were performed for each sample and the results are expressed as the average ± 0.01 error [11,12]. Microstructures of sintered alumina ceramics were examined by SEM (Hitachi S-4100, Tokyo, Japan) on thermally etched (1500 °C for 10 min) surfaces after coating with carbon for conductivity. The mechanical properties evaluated were hardness (H), fracture toughness (K_{Ic}) and flexural strength. Hardness was determined by applying a Vickers indenter and calculated as $H = P/2d^2$, d being the half-diagonal indentation impression and P the indentation load (10 kg). The flexural strength was measured using a 3-point bend test (JIS-R1601). Further, the fracture toughness value (K_{Ic}) was calculated on the basis of the indentation method [$K_{Ic} = Ha^{1/2} \times 0.203(C/a)^{-3/2}$] [15]. Here, $2a$ represents Vickers indent diagonal length, $2C$ the resulted crack length, and H is the Vickers hardness (H_V = kg/mm^2 = 10 MPa). Five to six samples were examined per case; in order to check the reproducibility of results and all the five readings were averaged out. The data of hardness, crack and diagonal length were collected using a micro-hardness tester (Leitz Wetzler, Germany) by holding the indenter tip (with 137°) under 10 kg load for 20 s on the surface of the sample polished to mirror finish. The results presented are the average of at least 25 indentations.

3. Results and discussion

Table 1 lists the dispersion media, powder composition, the viscosity of 50 vol.% solids loading suspensions measured at a shear rate ($\dot{\gamma}$) of 140 s^{-1}, the setting time, and compares the characteristics of green bodies consolidated by GC, HAS, and GCHAS with those of dry pressing samples obtained from the freeze dried granules.

It can be seen that viscosity at 140 s^{-1} seems to be more dependent on powder composition than on the dispersing medium. As a matter of fact viscosity decreased from 437 MPa s for GC to 141 MPa s 140 s^{-1} for GCHAS suspensions, which only differ on the added 4 wt.% of AlN (GCHAS). These results suggest that AlN enhances the fluidity of the suspension, especially when the pre-mix solution is used as dispersing medium. Besides a more favourable particle size

Table 1
Suspension characteristics and properties of green bodies consolidated by conventional dry pressing, aqueous gelcasting, hydrolysis assisted solidification, and hydrolysis induced aqueous gelcasting from suspensions containing 50 vol.% alumina.

Sample[a]	Suspension medium[b]	Starting powders		Suspension viscosity (mPa s at $\dot{\gamma} = 140\,s^{-1}$)	Suspension setting time (min)[c]	Density		Linear shrinkage upon drying (%)	Green strength (MPa)
		Al_2O_3 (wt.%)	AlN (wt.%)			Bulk (g/cm^3)	RD (%)[d]		
DP	H_2O	100	–	–	–	2.27 ± 0.13	57.0	–	<0.25
GC	CPM	100	–	437	~12 (30)	2.39 ± 0.16	60.1	2.4 ± 0.2	18.4 ± 1.4
HAS	H_2O	96	4	244	~1440	2.17 ± 0.19	54.5	1.6 ± 0.3	7.1 ± 2.0
GCHAS	NCPM	96	4	141	8.5 (30)	2.33 ± 0.12	58.8	1.7 ± 0.3	22.4 ± 2.2

[a] In the sample codes, DP, GC, HAS, and GCHAS stand for dry pressing, aqueous gelcasting, hydrolysis assisted solidification, and hydrolysis induced aqueous gelcasting, respectively.
[b] CPM stands for conventional pre-mix solution.
[c] The setting time for GC and GCHAS systems is the time corresponding to the crossover point ($G' = G''$). The values given in brackets represent the shortest time at which samples could be un-moulded.
[d] RD stands for relative density, assuming a theoretical density of 3.98 g/cm^3 for Al_2O_3.

distribution towards packing, this difference can also be due to some specific synergetic interactions, at least for short times of contact between AlN and water, which are not easy to discriminate in such a complex system.

The viscosity *versus* shear rate curves of GC and GCHAS (Table 1) are presented in Fig. 2. It can be seen that both suspensions exhibit shear thinning behaviours along the low shear rate range suitable for casting operations, i.e., up to $\dot{\gamma} \approx 75\,s^{-1}$, where a slight shear thickening trend starts to appear. The presence of some remaining agglomerated particles is the probable reason for the shear thickening behaviour exhibited by both the suspensions. The AlN containing suspension (i.e., GCHAS) is somewhat less viscous as can be seen from Table 1. Nevertheless, both suspensions exhibited viscosity values that are suitable for near-net-shaping of ceramics.

For longer contact times of AlN and water, AlN undergoes the following hydrolysis reactions (Eqs. (1)–(3)) [8]:

$$AlN + 2H_2O \rightarrow AlO(OH) + NH_3 \quad (1)$$

$$NH_3 + H_2O \rightarrow NH_4OH \quad (2)$$

$$AlO(OH) + H_2O \rightarrow Al(OH)_3 \quad (3)$$

Water consumption in all these reactions leads to an increase of solids volume fraction and a concomitant decrease of liquid available for flowing, which contributes to an increase in viscosity of suspension. Further, the release of ammonia tends to change pH towards the iso-electric point (IEP) of alumina, therefore, coagulating the suspension. Moreover, the formation of aluminium hydroxide as a reaction product from hydrolysis will act as cement bonding the alumina particles thereby stiffening the consolidating body [8].

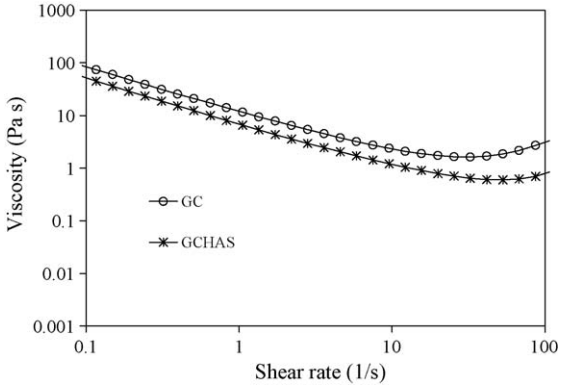

Fig. 2. Viscosity *vs.* shear rate of GC and GCHAS suspensions (details are available in Table 1).

The amount of NH_3 released upon hydrolysis of AlN and its kinetics should be kept under strict control to avoid the formation and entrapment of gas bubbles in the consolidating suspension, which will remain as pores in the green bodies. In the present case, the amount of NH_3 (1.67 wt.%, relative to the volume fraction of water) released upon hydrolysis of 4 wt.% AlN is well within the solubility limit of ammonia in water (at 20 °C, 31.34 mol% NH_3 per litre of water at STP, or ~532 g of NH_3 in 1000 g water). Therefore, the entrapment of gas bubbles in the green consolidates is not expected to occur to a great extent under these conditions [16].

The evolution of the internal structure of GCHAS suspension upon addition of polymerization initiator (APS) and catalyst (TEMED) is presented in Fig. 3 as a function of reaction time. Both the storage modulus or elastic component (G') and the loss modulus or viscous component (G'') increase with the increasing time. The viscous character predominates over the elastic one throughout the first period that starts with the addition of polymerization initiator and ends at the crossover point where $G' = G''$. The elapsed time up to this point is usually taken as the gelation time, above which the elastic character of the gelling systems predominates over the viscous one ($G' > G''$) by values that can go beyond more than two orders of magnitude. The GCHAS suspension took about 8.5–9 min to completely turn into a stiff gel upon addition of APS and TEMED. The setting/gelling of GC and HAS suspensions under ambient conditions upon addition of APS and TEMED, and upon hydrolysis of added AlN (4 wt.%), respectively, were accomplished in about 12 and 1440 min (24 h), respectively (Table 1). Due to the involvement of synergetic effect of both GC and HAS setting mechanisms the GCHAS system took a relatively shorter time for acquiring handling strength.

The mechanical spectra of the GC and GCHAS systems recorded under ambient temperature immediately after the

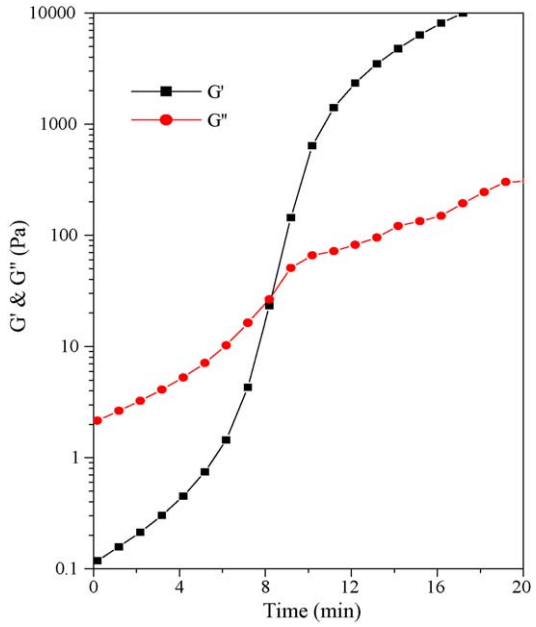

Fig. 3. Combined effects of free radical polymerization of organic monomers and AlN hydrolysis (4 wt.%) on the setting behaviour of GCHAS (details are given in Table 1).

crossover point are presented in Fig. 4. Due to the great differences in magnitude between G' and G'', the dynamic analysis was restricted to the elastic component only. In fact, under the tested conditions, the measurement of G'' is no longer reliable because it depends on the instrumental resolution of the phase lag between sinusoidal stress and strain [12]. Fig. 4 shows that both the curves run parallel to the x-axis, a characteristic behaviour of stiff gels. The body consolidated by GCHAS is much stiffer than the one obtained by GC. However, the latter gel is more stable over a frequency range of 0–100 Hz in comparison to the former one. The un-hydrolyzed AlN present in GCHAS gel could be undergone further hydrolysis upon increased frequency leading to changes in the gel stiffness. Nevertheless, the stiffness of the gels measured was found to be quite sufficient to fabricate thin wall near-net shape components such as radomes, domes, crucibles, etc. [8,12].

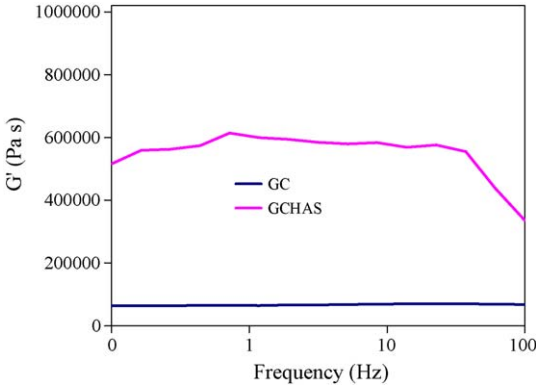

Fig. 4. Mechanical spectra measured immediately after the gelation time (crossover point of G' and G'') for consolidates derived from GC and GCHAS (details are given in Table 1).

Upon drying, the GC and GCHAS consolidates shrunk more in comparison to the one obtained by HAS. This difference is consistent with a more intricate 3D network of fine pores derived from the polymerization of organic monomers (i.e., MAM and MBAM) upon gelcasting. The higher capillary pressures developed in these finer pores is responsible for the higher sensitivity of gelcast bodies to drying [10,11], which are equivalent to a higher external pressure applied to consolidate during this processing step. Contrarily, the HAS setting mechanism involves a coagulation process driven by the shift of pH towards the iso-electric point of alumina, which is prone to generate a more open pore structure. Therefore, the expected magnitude of capillary forces developed upon drying the HAS consolidates is lower, explaining the observed smaller linear shrinkage values. Interestingly, all consolidates exhibit linear drying shrinkage values well below 3%, which was considered the upper limit range for safe fabricating complex-shaped ceramic components with near-net shape by gelcasting [6,7].

Green strength data reported in Table 1 show that the GC and GCHAS consolidates are stronger than those obtained by HAS. This was expected considering that the 3D polymerization of organic MAM and MBAM monomers leads to enhanced mechanical properties in comparison to those derived from the HAS setting mechanisms [7,8,12]. On the other hand, the bodies consolidated by GCHAS exhibited higher strength in comparison to those obtained by GC. This difference seems quite obvious considering the synergy of both strengthening mechanisms active in the GCHAS: (i) polymerization of organic MAM, and MBAM monomers; and, (ii) the cementing action of $Al(OH)_3$ formed by AlN hydrolysis. Accordingly, these are the highest green strength values ever reported for alumina ceramics [1–5]. Green bodies with strength of about 20 MPa can be machined to obtain desired dimensions so that the extensive and expensive post sintering machining operations can be minimized or even eliminated.

The green density values appear to be strongly dependent on the consolidation route adopted (Table 1 and Fig. 5). The following trend is observed in the relative density of green samples: GC (60.1%) > GCHAS (58.8%) > DP (57.0%) > HAS (54.5%). This sequence is closely related to the drying shrinkage since both depend on the 3D network of pores formed upon consolidation, as explained in the above paragraphs. The polymerization of organic monomers in GC (Fig. 5a) and GCHAS (Fig. 5c) led to more closely packed particles than in the case of HAS (Fig. 5b), which exhibits some pores (shown in circles).

The values of bulk density, apparent porosity, water absorption capacity, hardness, fracture toughness, and flexural strength of sintered (2 h, 1600 °C) alumina ceramics consolidated by the four processing routes are presented in Table 2 together with the percentage of linear shrinkage associated with sintering process. The following sequence can be established for relative density: GC (97.7%) > DP (97.6%) > GCHAS (94.5%) > HAS (91.2%). The lower values for the ceramics derived from suspensions with added AlN suggest that some gas bubbles (NH_3 released from hydrolysis of AlN) have been entrapped in the green bodies hindering a high sintered density

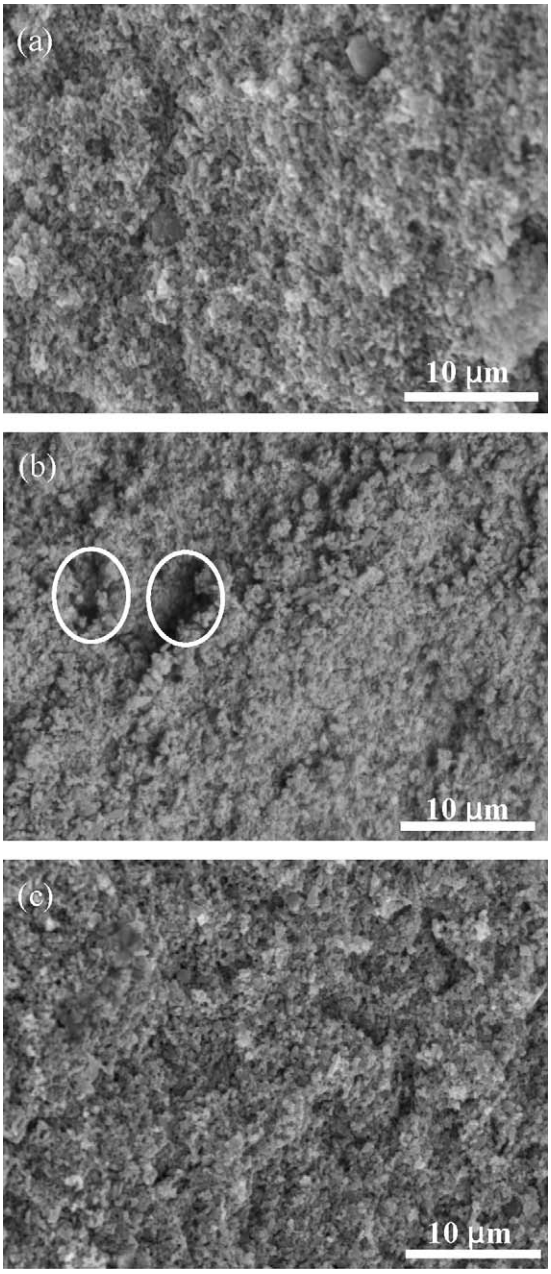

Fig. 5. SEM micrographs of green alumina bodies consolidated by: (a) GC; (b) HAS; and (c) GCHAS (details are given in Table 1).

to be achieved, pointing out to the need of a better balance between the kinetics of hydrolysis and of the overall setting of the suspensions.

All sintered samples exhibited apparent porosity and water absorption capacity values less than 0.312 and 0.002%, respectively. The highest linear shrinkage value (20.2%) was measured for the ceramics that achieved the highest degree of densification. According to Janney et al. [6], the total linear shrinkage associated with sintering of samples consolidated by colloidal processing routes should not exceed 25% to safely fabricate components with near-net shape. The data of sintered density, apparent porosity, and water absorption, presented in Table 2 are quite comparable with those reported for alumina ceramics consolidated by colloidal processing routes and sintered under similar conditions [5,18,19].

The measured hardness, fracture toughness and flexural strength appear to be highly dependent on the degree of densification achieved upon sintering (Table 2). It is known that the flexural strength and hardness properties are very sensitive to the presence of structural defects as pores. The highest values of hardness (1544 ± 19 kg/mm^2) and flexural strength (153 ± 21.0 MPa) consolidated by GC, which are not far from those consolidated by DP (1536 ± 34 kg/mm^2 and 142 ± 15 MPa); and the poorest mechanical properties of HAS ceramics (1394 ± 31 kg/mm^2 and 129.1 ± 30 MPa) confirm the expected trends. The GCHAS ceramics exhibit intermediate mechanical properties: (1476 ± 23 kg/mm^2, and 138.3 ± 13.0 MPa). The relatively low values of fracture toughness are certainly related to remaining pores that can be easily seen in the SEM micrographs presented in Fig. 6(a–d) for the GC, HAS, GCHAS and DP ceramics, respectively. All of them show equi-axed/hexagonal type grains in the size range of about 0.5–5 μm with intergranular pores. The HAS ceramics possess higher number of grains and grain boundaries for unit area, probably due to the small aluminium hydroxide particles formed upon hydrolysis. In general, GC and DP exhibit relatively large size grains (2–5 μm) in comparison to those observed in HAS and GCHAS ceramics in the range of about 0.5–3.5 μm. The larger grains of DP and GC together with their higher densification levels are certainly responsible for the higher measured hardness values. The flexural strength seems to be more influenced by the degree of densification rather than by the number of grains and grain boundaries present in the sintered microstructure. In line with sintered density values, GC

Table 2
Properties of sintered (2 h, 1600 °C) alumina ceramics consolidated by conventional dry pressing, aqueous gelcasting, hydrolysis assisted solidification, and hydrolysis induced aqueous gelcasting from suspensions containing 50 vol.% solids.

Sample[a]	Bulk density (g/cm^3)	RD (%)[b]	Apparent porosity (%)	Water absorption capacity (%)	Linear shrinkage (%)	Hardness (kg/mm^2)	Fracture toughness (MPa m$^{1/2}$)	Flexural strength (MPa)
DP	3.88	97.6	0.185	0.045	14.9 ± 0.1	1536 ± 34	2.5 ± 0.2	142 ± 15
GC	3.89	97.7	0.213	0.002	20.2 ± 0.1	1544 ± 19	2.6 ± 0.1	153 ± 21
HAS	3.63	91.2	0.244	0.058	17.3 ± 0.1	1394 ± 31	2.6 ± 0.2	129 ± 30
GCHAS	3.76	94.5	0.312	0.046	19.9 ± 0.1	1476 ± 23	2.5 ± 0.3	138 ± 13

[a] In the sample codes, DP, GC, HAS, and GCHAS stand for dry pressing, aqueous gelcasting, hydrolysis assisted solidification, and hydrolysis induced aqueous gelcasting, respectively.
[b] RD stands for relative density, assuming a theoretical density of 3.98 g/cm^3 for Al_2O_3.

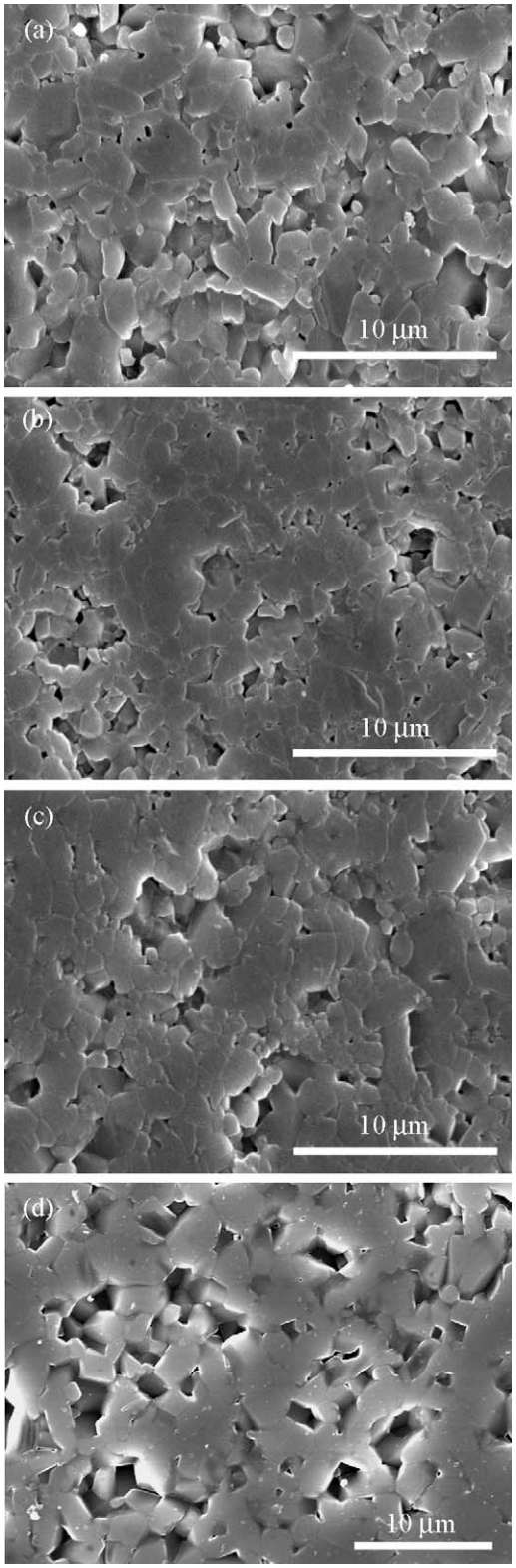

Fig. 6. SEM micrographs of (a) GC; (b) HAS; (c) GCHAS and (d) DP sintered for 2 h at 1600 °C (other details are given in Table 2).

has relatively less number of pores in comparison to other three samples. Nevertheless, the mechanical properties measured for these samples and the observed SEM microstructures are similar to the information reported for alumina ceramics consolidated by colloidal processing routes and sintered under similar conditions [17–19].

4. Conclusions

Dense alumina ceramics with near-net shape could be consolidated following hydrolysis induced aqueous gelcasting (GCHAS) of suspensions containing 50 vol.% solids loading. The yield of GCHAS process for producing alumina radome shapes with about 290 mm height and 125 mm base diameter from a suspension containing 50 vol.% solids was found to be more than 95%. The polyethylene glycol (PEG400) can be used to partly dry the wet-green radome shapes before removing them from the mould. The mechanical properties of sintered (1600 °C, 2 h) alumina ceramics consolidated by GCHAS can be compared very well with those of alumina ceramics consolidated by aqueous gelcasting (GC), hydrolysis assisted solidification (HAS), and by conventional dry pressing of freeze dried granules.

Acknowledgements

IG thanks SERC-DST (Government of India) for the awarded BOYSCAST fellowship (SR/BY/E-04/06). S.M. Olhero wishes to thank to Foundation for Science and Technology (FCT) of Portugal for the financial support under the grant SFRH/BPD/27013/2006. The financial support of CICECO is also acknowledged.

References

[1] W.H. Gitzen, Alumina as a ceramic material, Special Publication No. 4, Book published by the American Ceramic Society, 735 Ceramic Place, Westerville, Ohio 43081, 1970, ISBN 0-916094-46-4, and references therein.
[2] R. Antonsen, Hydrostatic pressing of alumina radomes, PB Report, 131565, U.S. Govt. Research Reports, 29 (3) (1958) 125.
[3] N.N. Ault, Z.H. Milligan, Alumina radomes by plasma-spray process, Am. Ceram. Soc. Bull. 38 (11) (1959) 661–664.
[4] D.B. Binns, The testing of alumina ceramics for engineering applications, J. Br. Ceram. Soc. 2 (1965) 294–308.
[5] J.M.F. Ferreira, Role of the clogging effect in the slip casting process, J. Eur. Ceram. Soc. 18 (1998) 1161–1169.
[6] M.A. Janney, S.D. Nunn, C.A. Walls, O.O. Omatete, R.B. Ogle, G.H. Kirby, A.D. McMillan, Gelcasting, in: M.N. Rahman (Ed.), The Handbook of Ceramic Engineering, Marcel Dekker, New York, 1998, pp. 1–15.
[7] I. Ganesh, Near-net shape β-$Si_4Al_2O_2N_6$ parts by hydrolysis induced aqueous gelcasting process, Int. J. Appl. Ceram. Technol. 6 (1) (2009) 89–101.
[8] T. Kosmac, S. Novak, M. Sajko, Hydrolysis-assisted solidification (HAS): a new setting concept for ceramic net-shaping, J. Eur. Ceram. Soc. 17 (1997) 427–432.
[9] L. Bergström, Method for forming ceramic powders by temperature induced flocculation, U.S. Patent 5,340,532, 23rd August 1994.
[10] I. Ganesh, S.M. Olhero, P.M.C. Torres, J.M.F. Ferreira, Gelcasting of $MgAl_2O_4$ spinel powder, J. Am. Ceram. Soc. 92 (2) (2009) 350–357.
[11] I. Ganesh, D.C. Jana, S. Shaik, N. Thiyagarajan, An aqueous gelcasting process for sintered silicon carbide ceramics, J. Am. Ceram. Soc. 89 (10) (2006) 3056–3064.
[12] I. Ganesh, S.M. Olhero, P.M.C. Torres, F.J. Alves, J.M.F. Ferreira, Hydrolysis induced aqueous gelcasting for near-net shape forming of ZTA ceramic composites, J. Eur. Ceram. Soc. 29 (2009) 1393–1401.

[13] I. Ganesh, J.J. Reddy, G. Sundararajan, S.M. Olhero, P.M.C. Torres, J.M.F. Ferreira, Influence of processing route on micro-structure and mechanical properties of $MgAl_2O_4$ spinel, Ceram. Int. 36 (2010) 473–482.
[14] M.A. Janney, C.A. Walls, D.M. Kupp, K.W. Kirby, Gelcasting SiAlON radomes, Am. Ceram. Soc. Bull. 7 (2004) 9201–9206.
[15] G.R. Anstis, P. Chantikul, B.R. Lawn, D.B. Marshall, A critical evaluation of indentation techniques for measuring fracture toughness. I. Direct crack measurements, J. Am. Ceram. Soc. 64 (1981) 533–538.
[16] I. Ganesh, N. Thiyagarajan, D.C. Jana, P. Barik, G. Sundararajan, J.M.F. Ferreira, Dense β-SiAlONs consolidated by a modified hydrolysis assisted solidification route, J. Eur. Ceram. Soc. 28 (4) (2008) 879–885.
[17] O. Lyckfeldt, J.M.F. Ferreira, Processing of porous ceramics by starch consolidation, J. Eur. Ceram. Soc. 18 (2) (1998) 131–140.
[18] S. Dhara, P. Bhargava, A simple direct casting route to ceramic foams, J. Am. Ceram. Soc. 86 (10) (2003) 1645–1650.
[19] I. Ganesh, P.M.C. Torres, J.M.F. Ferreira, Densification behavior of combustion derived Al_2O_3 powders, Ceram. Int. 35 (2009) 1173–1179.